Multi-Unimodular Waveform Design With Low Peak Sidelobe Level Via Direct Phase Optimizations

Xiaohan Zhao, Yongzhe Li, and Ran Tao
School of Information and Electronics, Beijing Institute of Technology, Beijing 100081, China
Emails: 3120215436@bit.edu.cn, lyz@ieee.org/yongzhe.li@bit.edu.cn, rantao@bit.edu.cn

***Abstract*—In this paper, we propose an efficient algorithm for designing multi-unimodular waveforms with low peak sidelobe level (PSL) toward any time lags of interest, which differs from existing approaches. The generic PSL metric defined on the TLOI is formulated for minimization, and the phase values of waveforms are directly optimized. To be specific, we first convert the PSL-minimization based waveform design into an l_p-norm based minimization problem. Then, we reformulate it into an unconstrained optimization problem with respect to the phase values of waveform elements, wherein the inherent waveform property of constant envelopes and a discrete Fourier transform matrix are both used. Our remaining contributions lie in deriving the complex gradient of the unconstrained objective and also elaborating its majorant via a Lipschitz-constant related quantity which is properly designed. A closed-form solution that updates the phase values through iterations is obtained by the majorization-minimization framework, and it boils down to a gradient descent regime. The fast implementation of our algorithm is also provided, whose performance improvements are verified.**

***Index Terms*—Multi-waveform design, peak sidelobe level (PSL), time lags of interest (TLOI), phase optimizations.**

I. Introduction

Waveform/code design has been attracting significant interest during the past decades [1]–[4], which plays an important role in radar [2], communications [5], active sensing [4], and coexistence of radar/sensing and communications [6], [7]. It is widely recognized as an essential key to ensure high-quality transmissions in these applications, which enables many advantages [8] such as improved identifiability of targets, better delay-Doppler ambiguities, increased robustness on estimations, etc. Conventionally, only a single waveform (or a code sequence) is to be designed, while the emergence of multi-input multi-output (MIMO) radar and its integration with communications in recent years has accelerated the research progress on waveform design to step into a new era.

There have already been some works on the waveform design in recent years [9]–[19], which are typically devised on the basis of optimizing certain criteria with respect to waveform aspects. Among such existing methods, the ones that focus on minimizing the integrated sidelobe level (ISL) [9]–[13] or peak sidelobe level (PSL) [14]–[19], or equivalently, minimizing the auto- and cross-correlation level of waveforms are most commonly adopted. In essence, the ISL- or PSL-minimization based waveform(s) design emphasizes on the principle that a bank of matched filters for multi-waveform applications can be implemented by the correlations between waveforms and their delayed replicas [4]. Such waveform design is typically suitable for the situation that receivers are fixed to be the matched filters, whose focus is solely the quality of waveform correlations. The major difference between the ISL- and PSL-minimization based designs is that the former deals with the reduction of accumulated sidelobes, while the latter devotes to suppressing the worst-case sidelobe for all time lags.

Regarding the PSL-minimization based waveform design, there are few works reported in public literature to optimally generate multiple unimodular waveform(s) [15]–[19]. The relevant works [15] and [16] mainly dealt with the case of single waveform at the early stage, whose algorithms suffer from high computational complexity and low convergence speed for waveform generation. The later works [17]–[19] developed in terms of this regime adapts to the case of multiple waveforms, but their performances are more subject to the same drawbacks as in the single-waveform case. Generally speaking, the algorithm developments of these works resort to iterations, each of which particularly involve repetitive projections of complex values into their constant-modulus approximations. This motivates us to devise new methods with advanced performances from the perspective of avoiding such redundant procedures. On the other hand, the aforementioned methods have no concentration on controlling the PSL only toward certain time lags that are of interest.

In this paper, we propose a fast and efficient algorithm for designing multi-unimodular waveforms with low PSL toward any time lags of interest (TLOI). The phase values of waveform elements are directly optimized, which successfully removes the repetitive projections of complex values into constant-modulus approximations used in existing approaches. We start from formulating a generic PSL metric defined on the TLOI for minimization, which is converted into an l_p-norm based minimization problem then. Our innovation is to reformulate the obtained design problem into an unconstrained optimization problem with respect to the phase values of waveform elements, wherein the inherent waveform property of constant envelopes and a discrete Fourier transform matrix are both used. Our remaining contributions lie in deriving the complex gradient of the unconstrained objective and also elaborating its majorant via a Lipschitz-constant related quantity which is properly designed. A closed-form solution that updates the phase values through iterations is obtained via majorization-minimization techniques [20], which boils down to a gradient descent regime. The fast implementation of our algorithm is provided, whose advantages over the current state-of-the-art methods are verified.

This work was supported in part by the National Natural Science Foundation of China (NSFC) under grants 62271054 and U21A20456.

Notations: We use $|\cdot|$, $\|\cdot\|$, $\|\cdot\|_\infty$, $(\cdot)^*$, $(\cdot)^{\mathrm{T}}$, $(\cdot)^{\mathrm{H}}$, $\odot$, ∇, ∇^2, $\max\{\cdot\}$, $\mathcal{O}(\cdot)$, $\mathbf{1}_M$, $\mathbf{0}_{P\times M}$, $\Re\{\cdot\}$, and $\Im\{\cdot\}$ to denote element-wise modulus, Euclidean norm, infinity norm, conjugate, transpose, conjugate transpose, Hadamard product, gradient, Hessian, maximum value of a vector, order of complexity, M-length vector of all ones, $(P\times M)$-dimensional matrix of all zeros, real part, and imaginary part, respectively. Moreover, operators $\mathbf{dom}(\cdot)$, $\mathbb{d}\{\cdot\}$, $\mathfrak{D}\{\cdot\}$, $\mathcal{F}_P\{\cdot\}$, $\mathcal{G}_P\{\cdot\}$ (or $\tilde{\mathcal{G}}_P\{\cdot\}$), and $\mathcal{T}\{\cdot,\cdot\}$ denote domain of a function, picking up the main diagonal elements of a matrix to form a vector, diagonalizing a vector, applying the $(2P-1)$-point fast Fourier transform (FFT) ($\mathcal{F}_P\{\cdot\}^{-1}$ for inverse FFT), truncating the first P (or the last P) elements of a vector, and constructing a Hermitian Toeplitz matrix whose first column and row coincide with the two input vectors in order, respectively.

II. Problem Formulation

Consider designing a set of M unimodular waveforms, each of which is of code length P. We store all the waveforms into a matrix denoted by $\mathbf{Y} \triangleq [\mathbf{y}_1,\ldots,\mathbf{y}_M]^{\mathrm{T}} \in \mathbb{C}^{P\times M}$, whose m-th column corresponds to the m-th waveform characterized by $\mathbf{y}_m \triangleq [e^{j\boldsymbol{\psi}_m(1)},\cdots,e^{j\boldsymbol{\psi}_m(P)}]^{\mathrm{T}} \in \mathbb{C}^{P\times 1}$. Here, $\boldsymbol{\psi}_m(p)$ denotes the phase value of the p-th element in $\mathbf{y}_m$, which arbitrarily ranges between 0 and 2π. For the purpose of later use, we also store all the phase values of each waveform into a vector, i.e., $\boldsymbol{\psi}_m \triangleq [\boldsymbol{\psi}_m(1),\cdots,\boldsymbol{\psi}_m(P)]^{\mathrm{T}} \in \mathbb{R}^{P\times 1}$, $\forall m \in \mathfrak{M}$ with $\mathfrak{M}$ defined as $\mathfrak{M} \triangleq \{1,\cdots,M\}$.

Without loss of generality, we denote $\mathfrak{P}$ as the set of TLOI, which can be any subset of $\{-P+1,\cdots,-1,1,\cdots,P-1\}$. Thus, the PSL defined on the TLOI $\mathfrak{P}$, denoted by ζ_{TLOI} can be expressed as

$$\zeta_{\mathrm{TLOI}} \triangleq \max_{p\in\mathfrak{P}}\{|r_{mm'}(p)|\},\ \forall m,m' \in \mathfrak{M} \tag{1}$$

where $r_{mm'}(p)$ is the cross-correlation between the m-th and m'-th waveforms at p-th time lag given as follows

$$r_{mm'}(p) \triangleq \sum_{k=p+1}^{P} \mathbf{y}_m(k)\mathbf{y}_{m'}^*(k-p) = r_{m'm}^*(-p),$$
$$\forall p \in \{1,...,P-1\}; m,m' \in \mathfrak{M}. \tag{2}$$

Hence, the PSL-minimization based waveform design defined on the TLOI $\mathfrak{P}$ can be formulated as

$$\begin{aligned} \min_{\mathbf{Y}}\quad & \zeta_{\mathrm{TLOI}} \\ \text{s.t.}\quad & |[\mathbf{Y}]_{m,p'}| = 1,\ m=1,\ldots,M;\ p'=1,\ldots,P. \end{aligned} \tag{3}$$

In order to solve (3), we convert the original PSL-minimization based waveform design to the form as follows

$$\begin{aligned} \min_{\mathbf{Y}}\quad & \Big(\sum_{p\in\mathfrak{P}}\sum_{\substack{m,m'\in\mathfrak{M}\\ m'\neq m}}|r_{mm'}(p)|^q\Big)^{\frac{1}{q}} \\ \text{s.t.}\quad & |[\mathbf{Y}]_{m,p'}| = 1,\ p'=1,\cdots,P \end{aligned} \tag{4}$$

where the q-th order norm has been employed to approximate ζ_{TLOI}. Note that the problem (4) is equivalent to (3) when q equals $+\infty$, and it boils down to the weighted ISL (WISL)-minimization based waveform design (see (42) of [11]) when q equals 2.

III. Efficient Multi-Unimodular Waveform Design via Direct Phase Optimizations

Let us store the correlations between $\mathbf{y}_m$ and $\mathbf{y}_{m'}$ at all time lags into a vector denoted by $\mathbf{r}_{m,m'} \in \mathbb{C}^{(2P-1)\times 1}$, i.e., $\mathbf{r}_{m,m'} \triangleq [r_{mm'}(-P+1),\cdots,r_{mm'}(0),\cdots,r_{mm'}(P-1)]^{\mathrm{T}}$. For the sake of reformulating (4) into a form composed of matrix-vector products, we also define $\boldsymbol{\gamma} \triangleq [\gamma_{-P+1},\cdots,\gamma_0,\cdots,\gamma_{P-1}] \in \mathbb{R}^{(2P-1)\times 1}$, whose elements are equal to 1 if their subscripts belong to the set $\mathfrak{P}$ while the others are all zeros. Moreover, we introduce a discrete Fourier transform (DFT) matrix $\mathbf{D} \in \mathbb{C}^{2P\times 2P}$, whose (p,p')-th element is given by $[\mathbf{D}]_{p,p'} \triangleq e^{-j\frac{2\pi}{2P}(p-1)(p'-1)}$.

Using the fact that $\mathbf{r}_{mm'} = \frac{1}{2P}\mathbf{J}_2^{\mathrm{T}}\mathbf{D}^*((\mathbf{D}\mathbf{J}_1^{\mathrm{T}}\mathbf{y}_m)\odot(\mathbf{D}^*\mathbf{J}_1^{\mathrm{T}}\mathbf{y}_{m'}^*))$, with $\mathbf{J}_1$ and $\mathbf{J}_2$ defined as $\mathbf{J}_1 \triangleq [\mathbf{I}_P,\mathbf{0}_P] \in \mathbb{R}^{2P\times P}$ and $\mathbf{J}_2 = \begin{bmatrix} \mathbf{0}_{(P+1)\times(P-1)} & \mathbf{I}_P \\ \mathbf{I}_{P-1} & \mathbf{0}_{P\times P} \end{bmatrix} \in \mathbb{R}^{2P\times(2P-1)}$, respectively, the problem (4) can be rewritten as follows

$$\begin{aligned} \min_{\mathbf{Y}}\quad & \frac{1}{2P}\Bigg(\sum_{\substack{m,m'\in\mathfrak{M}\\ m'\neq m}}\big(|((\mathbf{y}_m^{\mathbf{T}}\mathbf{J}_1\mathbf{D})\odot(\mathbf{y}_{m'}^{\mathrm{H}}\mathbf{J}_1\mathbf{D}^*))\mathbf{D}^*\mathbf{J}_2|^q \\ & \qquad\qquad \odot\boldsymbol{\gamma}^{\mathrm{T}}\big)\mathbf{1}_{2P-1}\Bigg)^{\frac{1}{q}} \\ \text{s.t.}\quad & |[\mathbf{Y}]_{m,p'}| = 1,\ p'=1,\cdots,P. \end{aligned} \tag{5}$$

Ignoring the constant scalar $\frac{1}{2P}$ and also the power $\frac{1}{q}$ which are immaterial to optimization, substituting $\mathbf{y}_m = e^{j\boldsymbol{\psi}_m}$, $\forall m \in \mathfrak{M}$ to (5),[1] the PSL-minimization based waveform design can be further rewritten as

$$\begin{aligned} \min_{\mathbf{Y}}\quad & \sum_{\substack{m,m'\in\mathfrak{M}\\ m'\neq m}}\big(\big|(((e^{j\boldsymbol{\psi}_m})^{\mathbf{T}}\mathbf{J}_1\mathbf{D})\odot((e^{j\boldsymbol{\psi}_{m'}})^{\mathrm{H}}\mathbf{J}_1\mathbf{D}^*))\mathbf{D}^*\mathbf{J}_2\big|^q \\ & \qquad\qquad \odot\boldsymbol{\gamma}^{\mathrm{T}}\big)\mathbf{1}_{2P-1} \end{aligned} \tag{6}$$

which is an unconstrained optimization problem with respect to $\boldsymbol{\psi}$ that consists of all the phase values of waveform elements.

In order to solve (6), we employ the idea of finding a proper majorant for its objective, and then solve the resulting problem by means of majorization-minimization techniques. Before proceeding with (6), we present the following result.

Lemma 1. *If a real-valued function $f(\mathbf{x})$ with respect to a real variable $\mathbf{x}$ is second-order differentiable, and there is a constant L satisfying $L \geq \|\nabla f(\boldsymbol{x}) - \nabla f(\boldsymbol{z})\|/\|\boldsymbol{x}-\boldsymbol{z}\|$, $\forall \mathbf{x},\mathbf{z} \in \mathbf{dom}(f)$ with $\mathbf{x}\neq\mathbf{z}$, then the following function*

$$g(\mathbf{x}) = f(\mathbf{x}_0) + (\nabla f(\mathbf{x}_0))^{\mathrm{T}}(\mathbf{x}-\mathbf{x}_0) + \frac{L}{2}\|\mathbf{x}-\mathbf{x}_0\|^2 \tag{7}$$

can serve as a majorant for $f(\mathbf{x})$ at any given $\mathbf{x}_0 \in \mathbf{dom}(f)$.

Proof. Using Lemma 1.2.3 of [21], we can obtain that $\big|f(\mathbf{x}) - f(\mathbf{x}_0) - (\nabla f(\mathbf{x}_0))^{\mathrm{T}}(\mathbf{x}-\mathbf{x}_0)\big| \leq \frac{L}{2}\|\mathbf{x}-\mathbf{x}_0\|^2$, which leads to the fact that $f(\mathbf{x}) - f(\mathbf{x}_0) - (\nabla f(\mathbf{x}_0))^{\mathrm{T}}(\mathbf{x}-\mathbf{x}_0) \leq \frac{L}{2}\|\mathbf{x}-\mathbf{x}_0\|^2$, thereby enabling $g(\mathbf{x}) \geq f(\mathbf{x})$, $\forall \mathbf{x} \in \mathbf{dom}(f)$, $g(\mathbf{x}_0) = f(\mathbf{x}_0)$, and $\nabla g(\mathbf{x})|_{\mathbf{x}=\mathbf{x}_0} = \nabla f(\mathbf{x})|_{\mathbf{x}=\mathbf{x}_0}$ to hold. The proof is complete. □

[1] Here, the exponential function $e^{j(\cdot)}$ is applied to a vector argument, whose calculation is conducted in terms of each element of the input vector. The same type of operations for $\Re\{\cdot\}$, $\Im\{\cdot\}$, and $|\cdot|$ is used in the paper.

Let us denote the objective of (6) as $\zeta(\boldsymbol{\psi})$, which is to be used in the following. To apply Lemma 1 to $\zeta(\boldsymbol{\psi})$ for the elaboration of its majorant, we need to determine its gradient and to find the constant L which is desired to be easily obtained. Toward this end, we present the following results.

Lemma 2. *The gradient of $\zeta(\boldsymbol{\psi})$, denoted by $\nabla\zeta(\boldsymbol{\psi})$, can be obtained as $\nabla\zeta(\boldsymbol{\psi}) = [\nabla_1\zeta(\boldsymbol{\psi})^{\mathrm{T}}, \cdots, \nabla_M\zeta(\boldsymbol{\psi})^{\mathrm{T}}]^{\mathrm{T}}$, whose m-th component is given as follows*

$$\nabla_m\zeta(\boldsymbol{\psi}) = 2q\sum_{m'=1}^{M}\Im\Big\{\mathbf{J}_1\mathbf{D}\big(\mathbf{D}^*\mathbf{J}_2(\mathbf{r}^*_{m,m'}\odot|\mathbf{r}_{m,m'}|^{q-2}\odot\boldsymbol{\gamma}) \odot\big(\mathbf{D}\mathbf{J}_1^{\mathrm{T}}e^{j\boldsymbol{\psi}_{m'}}\big)\big)\odot e^{-j\boldsymbol{\psi}_m}\Big\} \tag{8}$$

with $\boldsymbol{\psi}_m \in \mathbb{R}^{P\times 1}$ (or $\boldsymbol{\psi}_{m'} \in \mathbb{R}^{P\times 1}$) being the m-th (or m'-th) phase vector that has been defined at the beginning of Sec. II

Proof. Due to the fact $|\mathbf{r}_{m,m'}|^2 = \Re\{\mathbf{r}_{m,m'}\}^2 + \Im\{\mathbf{r}_{m,m'}\}^2$, we can expand $\zeta(\boldsymbol{\psi})$ and express its gradient with respect to the m-th phase vector as

$$\begin{aligned}\nabla_m\zeta(\boldsymbol{\psi}) = q\sum_{m'=1}^{M}\big(&\Im\big\{\mathfrak{D}\{e^{-j\boldsymbol{\psi}_m}\}\mathbf{J}_1\mathbf{D}^*\mathfrak{D}\{\mathbf{D}\mathbf{J}_2^{\mathrm{T}}e^{j\boldsymbol{\psi}_m}\}\\ &\mathbf{D}^*\mathbf{J}_2\big\}\mathfrak{D}\{\Re\{\mathbf{r}_{m,m'}\}\} - \Re\{\mathfrak{D}\{e^{-j\boldsymbol{\psi}_m}\}\mathbf{J}_1\mathbf{D}^*\mathfrak{D}\{\mathbf{D}\mathbf{J}_2^{\mathrm{T}}e^{j\boldsymbol{\psi}_m}\}\\ &\mathbf{D}^*\mathbf{J}_2\}\mathfrak{D}\{\Im\{\mathbf{r}_{m,m'}\}\}\big)\mathfrak{D}\{\boldsymbol{\gamma}\odot|\mathbf{r}_{m,m'}|^{q-2}\}\mathbf{1}_{2P-1},\end{aligned} \tag{9}$$

which can be further rewritten as (8) via the facts that $\Im\big\{\mathfrak{D}\{e^{-j\boldsymbol{\psi}_m}\}\mathbf{J}_1\mathbf{D}^*\mathfrak{D}\{\mathbf{D}\mathbf{J}_2^{\mathrm{T}}e^{j\boldsymbol{\psi}_m}\}\mathbf{D}^*\mathbf{J}_2\big\}\mathfrak{D}\{\Re\{\mathbf{r}_{m,m'}\}\} - \Re\{\mathfrak{D}\{e^{-j\boldsymbol{\psi}_m}\}\mathbf{J}_1\mathbf{D}^*\mathfrak{D}\{\mathbf{D}\mathbf{J}_2^{\mathrm{T}}e^{j\boldsymbol{\psi}_m}\}\mathbf{D}^*\mathbf{J}_2\}\mathfrak{D}\{\Im\{\mathbf{r}_{m,m'}\}\} = \Im\{\mathfrak{D}\{e^{-j\boldsymbol{\psi}_m}\}\mathbf{J}_1\mathbf{D}\mathfrak{D}\{\mathbf{D}^*\mathbf{J}_2^{\mathrm{T}}e^{-j\boldsymbol{\psi}_m}\}\mathbf{D}\mathbf{J}_2\mathfrak{D}\{\mathbf{r}_{m,m'}\}\}$ and $\mathfrak{D}\{\mathbf{r}_{m,m'}\}\mathfrak{D}\{\boldsymbol{\gamma}\odot|\mathbf{r}_{m,m'}|^2\}\mathbf{1}_{2P-1} = \mathbf{r}_{m,m'}\odot|\mathbf{r}_{m,m'}|^2\odot\boldsymbol{\gamma}$. The proof is complete. □

Lemma 3. *The following quantity*

$$\begin{aligned}L(\boldsymbol{\psi}) = 2q\max_m\Bigg\{\Bigg|(4P-2)(q-1)\Bigg\|\sum_{m'=1}^{M}\Re\big\{|\mathfrak{D}\{e^{-j\boldsymbol{\psi}_m}\}\mathbf{J}_1\mathbf{D}\\ \mathfrak{D}\{\mathbf{D}^*\mathbf{J}_2^{\mathrm{T}}e^{-j\boldsymbol{\psi}_m}\}\mathbf{D}\mathbf{J}_2|^2\mathfrak{D}\big\{\boldsymbol{\gamma}\odot|\mathbf{r}_{m,m'}|^{q-2}\big\}\mathbf{1}_{2P-1}\big\}\Bigg\|_\infty\\ -\sum_{m'=1}^{M}\Re\Big\{\mathbf{J}_1^*\mathbf{D}^*\big(\mathbf{D}^*\mathbf{J}_2(\mathbf{r}^*_{m,m'}\odot|\mathbf{r}_{m,m'}|^{q-2}\odot\boldsymbol{\gamma})\\ \odot(\mathbf{D}\mathbf{J}_1^{\mathrm{T}}e^{j\boldsymbol{\psi}_{m'}})\big)\odot e^{-j\boldsymbol{\psi}_m}\Big\} + \frac{2^q\gamma_0^qP^{2q-1}}{(2P-1)^{q-1}}\Bigg|\Bigg\}\end{aligned} \tag{10}$$

ensures $g(\boldsymbol{\psi})|_{L=L(\boldsymbol{\psi})}$ to majorize $\zeta(\boldsymbol{\psi})$ at any given $\boldsymbol{\psi}^{(k)}$, where $g(\boldsymbol{\psi})$ is constructed by (7) of Lemma 1.

Proof. In terms of Lemma 1, the condition that Lemma 3 holds is to show that $L(\boldsymbol{\psi}) \geq \big\|\nabla\zeta(\boldsymbol{\psi}^+) - \nabla\zeta(\boldsymbol{\psi}^-)\big\|/\big\|\boldsymbol{\psi}^+ - \boldsymbol{\psi}^-\big\|$, $\forall\boldsymbol{\psi}^+, \boldsymbol{\psi}^- \in \mathbf{dom}(\zeta)$ with $\boldsymbol{\psi}^+ \neq \boldsymbol{\psi}^-$. Note that

$$\begin{aligned}\frac{\big\|\nabla\zeta(\boldsymbol{\psi}^+) - \nabla\zeta(\boldsymbol{\psi}^-)\big\|}{\big\|\boldsymbol{\psi}^+ - \boldsymbol{\psi}^-\big\|} &\leq \max_{p'}\left\{\left|\frac{\frac{\partial\zeta(\boldsymbol{\psi}^+)}{\partial\boldsymbol{\psi}^+(p')} - \frac{\partial\zeta(\boldsymbol{\psi}^-)}{\partial\boldsymbol{\psi}^-(p')}}{\boldsymbol{\psi}^+(p') - \boldsymbol{\psi}^-(p')}\right|\right\}\\ &= \max_{p'}\left\{\left|\frac{\partial^2\zeta(\boldsymbol{\psi})}{\partial^2\boldsymbol{\psi}(p')}\right|\right\} = \max\big\{\,\big|\mathrm{d}\big\{\nabla^2\zeta(\boldsymbol{\psi})\big\}\big|\,\big\}\end{aligned} \tag{11}$$

where p' is an index of the vector elements found by the maximization on the right hand side of the inequality. Note that the first inequality of (11) holds due to the fact that $\|\mathbf{a}\| \leq \|\mathbf{b}\|\cdot\max_{p'}\{|\mathbf{a}(p')/\mathbf{b}(p')|\}$, $\forall\mathbf{a},\mathbf{b}\in\mathbb{R}^{MP\times 1}$ by enforcing $\mathbf{a} \triangleq \nabla\zeta(\boldsymbol{\psi}^+) - \nabla\zeta(\boldsymbol{\psi}^-)$ and $\mathbf{b} \triangleq \boldsymbol{\psi}^+ - \boldsymbol{\psi}^-$, respectively. The subsequent (first) equality is obtained by means of the *Mean Value Theorem* [22] with $\boldsymbol{\psi}(p')$ being some phase value in between $\boldsymbol{\psi}^-(p')$ and $\boldsymbol{\psi}^+(p')$, and the last equality simply holds due to the definition of the Hessian matrix $\nabla^2\zeta(\boldsymbol{\psi}) \in \mathbb{R}^{MP\times MP}$ and its diagonal elements.

Let $\{\nabla^2_m\zeta(\boldsymbol{\psi})\}_{m=1}^M \in \mathbb{R}^{P\times P}$ be the M block matrices on the main diagonal of $\nabla^2\zeta(\boldsymbol{\psi})$. Based on (9), we can express the diagonal of the m-th block $\nabla^2_m\zeta(\boldsymbol{\psi})$ in the form as follows

$$\begin{aligned}\mathrm{d}\big\{\nabla^2_m\zeta(\boldsymbol{\psi})\big\} = 2q\sum_{m'=1}^{M}\big((q-2)\big|\Im\big\{\mathfrak{D}\{e^{-j\boldsymbol{\psi}_m}\}\mathbf{J}_1\mathbf{D}^*\mathfrak{D}\{\mathbf{D}\\ \times\mathbf{J}_2^{\mathrm{T}}e^{j\boldsymbol{\psi}_m}\}\mathbf{D}^*\mathbf{J}_2\mathfrak{D}\{\mathbf{r}^*_{m,m'}\}\big\}\big|^2\mathfrak{D}\big\{\boldsymbol{\gamma}\odot|\mathbf{r}_{m,m'}|^{q-4}\big\}\mathbf{1}_{2P-1}\\ -\Re\big\{|\mathfrak{D}\{e^{-j\boldsymbol{\psi}_m}\}\mathbf{J}_1\mathbf{D}\mathfrak{D}\{\mathbf{D}^*\mathbf{J}_2^{\mathrm{T}}e^{-j\boldsymbol{\psi}_m}\}\mathbf{D}\mathbf{J}_2|^2\mathfrak{D}\big\{\boldsymbol{\gamma}\\ \odot|\mathbf{r}_{m,m'}|^{q-2}\big\}\mathbf{1}_{2P-1}\big\} + \Re\big\{|\mathfrak{D}\{e^{-j\boldsymbol{\psi}_m}\}\mathbf{J}_1\mathbf{D}\mathfrak{D}\{\mathbf{D}^*\mathbf{J}_2^{\mathrm{T}}e^{-j\boldsymbol{\psi}_m}\}\\ \times\mathbf{D}\mathbf{J}_2|^2\mathfrak{D}\big\{\boldsymbol{\gamma}\odot|\mathbf{r}_{m,m'}|^{q-2}\big\}\mathbf{1}_{2P-1}\big\}\big) + \frac{2^{q+1}q\gamma_0^qP^{2q-1}}{(2P-1)^{q-1}}\mathbf{1}_P.\end{aligned} \tag{12}$$

Using (12), we can then enlarge the last term of (11) as

$$\begin{aligned}&\max\big\{\,\big|\mathrm{d}\big\{\nabla^2\zeta(\boldsymbol{\psi})\big\}\big|\,\big\} = \max_m\big\{\big|\mathrm{d}\,\big\{\nabla^2_m\zeta(\boldsymbol{\psi})\big\}\big|\big\}\\ &\leq 2q\max_m\Bigg\{\Bigg|(4P-2)(q-1)\Bigg\|\sum_{m'=1}^{M}\Re\big\{|\mathfrak{D}\{e^{-j\boldsymbol{\psi}_m}\}\mathbf{J}_1\mathbf{D}\\ &\mathfrak{D}\{\mathbf{D}^*\mathbf{J}_2^{\mathrm{T}}e^{-j\boldsymbol{\psi}_m}\}\mathbf{D}\mathbf{J}_2|^2\mathfrak{D}\big\{\boldsymbol{\gamma}\odot|\mathbf{r}_{m,m'}|^{q-2}\big\}\mathbf{1}_{2P-1}\big\}\Bigg\|_\infty\\ &-\sum_{m'=1}^{M}\Re\Big\{\mathbf{J}_1^*\mathbf{D}^*\big(\mathbf{D}^*\mathbf{J}_2(\mathbf{r}^*_{m,m'}\odot|\mathbf{r}_{m,m'}|^{q-2}\odot\boldsymbol{\gamma})\\ &\odot(\mathbf{D}\mathbf{J}_1^{\mathrm{T}}e^{j\boldsymbol{\psi}_{m'}})\big)\odot e^{-j\boldsymbol{\psi}_m}\Big\} + \frac{2^q\gamma_0^qP^{2q-1}}{(2P-1)^{q-1}}\Bigg|\Bigg\} \triangleq L(\boldsymbol{\psi})\end{aligned} \tag{13}$$

wherein the results $\sum_{m'=1}^M\big|\Im\big\{\mathfrak{D}\{e^{-j\boldsymbol{\psi}_m}\}\mathbf{J}_1\mathbf{D}^*\mathfrak{D}\{\mathbf{D}\mathbf{J}_2^{\mathrm{T}}e^{j\boldsymbol{\psi}_m}\}\mathbf{D}^*\mathbf{J}_2\mathfrak{D}\{\mathbf{r}^*_{m,m'}\}\big\}\big|^2\mathfrak{D}\big\{\boldsymbol{\gamma}\odot|\mathbf{r}_{m,m'}|^{q-4}\big\}\mathbf{1}_{2P-1} \leq \sum_{m'=1}^M\Re\big\{|\mathfrak{D}\{e^{-j\boldsymbol{\psi}_m}\}\mathbf{J}_1\mathbf{D}\mathfrak{D}\{\mathbf{D}^*\mathbf{J}_2^{\mathrm{T}}e^{-j\boldsymbol{\psi}_m}\}\mathbf{D}\mathbf{J}_2|^2\mathfrak{D}\big\{\boldsymbol{\gamma}\odot|\mathbf{r}_{m,m'}|^{q-2}\big\}\mathbf{1}_{2P-1}\big\}$ have been used. The proof is complete. □

Till now, using Lemmas 1, 2, and 3, we can write the majorant for the objective of (6) as

$$g(\boldsymbol{\psi}) = \frac{L^{(k)}}{2}\boldsymbol{\psi}^{\mathrm{T}}\boldsymbol{\psi} + \Big(\nabla\zeta(\boldsymbol{\psi})|_{\boldsymbol{\psi}=\boldsymbol{\psi}^{(k)}} - L^{(k)}\Big)^{\mathrm{T}}\boldsymbol{\psi} + \mathrm{const} \tag{14}$$

where the last sum component represents constant terms irrelevant to $\boldsymbol{\psi}$, which is therefore immaterial to optimization, $\boldsymbol{\psi}^{(k)}$ denotes the vector of phase values obtained at the last (denoted by the k-th) iteration, $\nabla\zeta(\boldsymbol{\psi})|_{\boldsymbol{\psi}=\boldsymbol{\psi}^{(k)}}$ is the gradient of $\zeta(\boldsymbol{\psi})$ at $\boldsymbol{\psi}^{(k)}$ obtained by Lemma 2, and $L^{(k)} \triangleq L(\boldsymbol{\psi}^{(k)})$ is obtained by (13). Therefore, ignoring the constant terms of (14), we can rewrite the optimization problem (6) as

$$\min_{\boldsymbol{\psi}}\quad\frac{L^{(k)}}{2}\boldsymbol{\psi}^{\mathrm{T}}\boldsymbol{\psi} + \Big(\nabla\zeta(\boldsymbol{\psi})|_{\boldsymbol{\psi}=\boldsymbol{\psi}^{(k)}} - L^{(k)}\boldsymbol{\psi}^{(k)}\Big)^{\mathrm{T}}\boldsymbol{\psi} \tag{15}$$

Algorithm 1 The proposed PSL-minimization based waveform design via direct phase optimizations

1: Input: P, M, $\boldsymbol{\psi}^{(0)}$, $k \leftarrow 0$
2: **repeat**
3: Calculate $\{\nabla_m \zeta(\boldsymbol{\psi}^{(k)})\}_{m=1}^{M}$, $L^{(k)}$, and $\boldsymbol{\psi}^{(k+1)}$ via (16)-(18)
4: k=k+1
5: **until** convergence
6: Output: $\mathbf{y} = e^{j\boldsymbol{\psi}^{(k+1)}}$

which leads to the closed-form solution given by

$$\boldsymbol{\psi}^{(k+1)} = \boldsymbol{\psi}^{(k)} - \frac{1}{L^{(k)}} \nabla \zeta(\boldsymbol{\psi})|_{\boldsymbol{\psi}=\boldsymbol{\psi}^{(k)}}. \tag{16}$$

Note that (16) essentially boils down to the regime of *gradient descent method* with a proper step size equaling $1/L^{(k)}$.[2]

The calculation of (16) can be reduced by the fast implementation of $\nabla_m \zeta(\boldsymbol{\psi}^{(k)})$ and $L^{(k)}$ using FFT, i.e.,

$$\nabla_m \zeta(\boldsymbol{\psi}^{(k)}) = 2q \frac{(2P)^q}{(2P-1)^q} \sum_{m'=1}^{M} \Im\{\tilde{\mathcal{G}}_P\{\mathcal{F}_P^{-1}\{\mathcal{F}_P\{e^{j\boldsymbol{\psi}_{m'}^{(k)}}\} \odot \mathcal{F}_P^*\{\mathbf{r}_{m,m'} \odot \boldsymbol{\gamma} \odot |\mathbf{r}_{m,m'}|^{q-2}\}\}\} \odot \mathcal{F}_P^*\{e^{-j\boldsymbol{\psi}_m^{(k)}}\}\} \tag{17}$$

$$L^{(k)} = 2q \frac{(2P)^q}{(2P-1)^q} \max_m \Bigg\{ \Bigg| (4P-2)(q-1) \Bigg\| \sum_{m'=1}^{M} \tilde{\mathcal{G}}_P\{ \mathcal{F}_P^{-1}\{\mathcal{F}_P\{\boldsymbol{\gamma} \odot |\mathbf{r}_{m,m'}|^{q-2}\} \odot \mathcal{F}_P\{\mathbf{z}_P\}\}\} \Bigg\|_\infty - \sum_{m'=1}^{M} \Re\{\tilde{\mathcal{G}}_P\{ \mathcal{F}_P^{-1}\{\mathcal{F}_P\{e^{j\boldsymbol{\psi}_{m'}^{(k)}}\} \odot \mathcal{F}_P^*\{\mathbf{r}_{m,m'} \odot \boldsymbol{\gamma} \odot |\mathbf{r}_{m,m'}|^{q-2}\}\} \odot \mathcal{F}_P^*\{e^{-j\boldsymbol{\psi}_m^{(k)}}\}\} + (2P-1)\gamma_0^q P^{q-1} \Bigg| \Bigg\} \tag{18}$$

where the fact $\sum_{m'=1}^{M} \Re\{|\mathfrak{D}\{e^{-j\boldsymbol{\psi}_m}\}\mathbf{J}_1 \mathbf{D}\mathfrak{D}\{\mathbf{D}^* \mathbf{J}_2^{\mathrm{T}} e^{-j\boldsymbol{\psi}_m}\} \mathbf{D}\mathbf{J}_2|^2 \mathfrak{D}\{\boldsymbol{\gamma} \odot |\mathbf{r}_{m,m'}|^{q-2}\}\mathbf{1}_{2P-1}\} = 4P^2 \|\sum_{m'=1}^{M} \mathcal{T}\{\mathcal{G}_P\{\boldsymbol{\gamma} \odot |\mathbf{r}_{m,m'}|^{q-2}\}, \tilde{\mathcal{G}}_P\{\boldsymbol{\gamma} \odot |\mathbf{r}_{m,m'}|^{q-2}\}\mathbf{1}_P\|_\infty$ has been used, and $\mathbf{z}_P \triangleq [\mathbf{1}_P^{\mathrm{T}}, \mathbf{0}_{(P-1)\times 1}^{\mathrm{T}}]^{\mathrm{T}} \in \mathbb{R}^{(2P-1)\times 1}$. Hence, the overall computational complexity of (16) is reduced to $\mathcal{O}(M^2 P \log P)$. The corresponding procedures are summarized in Algorithm 1.

IV. Simulations

In this section, we evaluate the performance of our proposed algorithm and compare it with algorithms 'CAN' [9], 'MM-WeCorr' [10], 'ISLNew' [11], and 'MM-PSL' [15], respectively. Throughout simulations, random phase values are generated as initializations, and the same initialization is employed to conduct comparisons. Moreover, we apply FFT to the compared algorithms on the condition that they allow for fast implementations. The stopping criterion is chosen as the absolute PSL difference between two neighboring iterations normalized by the initial PSL value.

[2]The same type of conclusions for the WISL-minimization based waveform design can be found in [12].

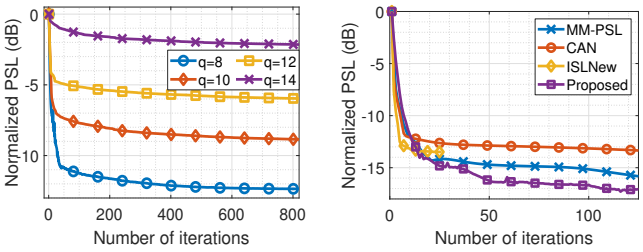

(a) Convergence speeds of our algorithm: $q = 8, 10, 12$, and 14.
(b) Convergence speeds of the tested algorithms: $q = 3$.

Fig. 1: The evaluation on the performance of convergence speeds.

Example 1: Evaluation on convergence speeds. We evaluate the convergence speed performance of our proposed algorithm in terms of normalized PSL values versus numbers of iterations. Different orders q chosen from $\{8, 10, 12, 14\}$ are tested to show its effect on the convergence speed of our algorithm, and the same order ($q = 3$) is used when comparing with other algorithms. The TLOI is set to be $[-19, -1] \cup [1, 19]$, and the tolerance for stopping iterations is set to be 10^{-7}. Corresponding results are shown in Fig. 1. It can be seen from Fig. 1(a) that our proposed algorithm converges after iterations for all tested orders, whose convergence speed becomes slower when the order increases. For the comparisons with other algorithms, it can be seen from Fig. 1(b) that our proposed algorithm iterates to the lowest PSL value after convergence, which has reached -17.05 dB. The algorithm CAN obtains the worst PSL after convergence, which is about -13.33 dB. Among the tested algorithms, ISLNew costs the least number of iterations, but it obtains relatively higher PSL value. The algorithm MM-PSL behaves the second best.

Example 2: Correlation evaluation. We compare normalized auto- and cross-correlation levels for all algorithms that are tested. The parameters $M = 2$, $P = 128$, and $q = 3$ are chosen, and the TLOI is set to be $[-127, -1] \cup [1, 127]$. The tolerance for stopping is set to be 10^{-9}. Other parameters are the same as used in the previous. It can be seen from Fig. 2 that our proposed algorithm outperforms all the other algorithms that are compared. The largest gap of the obtained PSL between our proposed algorithm and the others is about 8.01 dB, while the smallest gap is about 5.93 dB.

Example 3: PSL evaluation. We evaluate the PSL performance in terms of the minimum and average PSL values obtained after convergence, number of iterations, and time consumption, wherein all the results are averaged over 50 independent trials. The code lengths chosen from the set $\{512, 1024, 2048, 4096, 8193\}$ are tested, and the TLOI is set to be the same as in the second example. The tolerance parameter is set to be 10^{-6}. Other parameters are: $M = 1$ and $q = 3$. The corresponding results are shown in Table I. It can be seen that our proposed algorithm obtains the lowest minimum and average PSL values for all the tested code lengths. The average PSL values obtained by our proposed algorithm is about 1.198 dB, 12.079 dB, and 16.765 dB better than those obtained by MM-PSL, ISLNew, and CAN, respectively. In addition, our proposed algorithm shows the largest improvements on the time consumption using the least number of iterations for the

TABLE I: PSL performance of the algorithms tested versus different code lengths.

	$P = 512$				$P = 1024$				$P = 2048$				$P = 4096$				$P = 8192$			
	Min.[a]	Ave.[b]	Iter.[c]	Time[d]	Min.	Ave.	Iter.	Time	Min.	Ave.	Iter.	Time	Min.	Ave.	Iter.	Time	Min.	Ave.	Iter.	Time
MM-PSL	7.154	8.715	312	0.375	11.080	12.954	374	0.640	16.380	18.861	366	1.028	25.689	29.353	279	1.288	36.873	41.875	346	2.820
ISLNew	8.946	11.117	145	0.065	13.532	16.116	174	0.209	21.448	24.730	210	0.259	29.880	36.027	214	0.809	46.305	53.133	227	1.471
CAN	10.030	12.547	931	0.579	14.799	18.511	1217	1.501	22.455	26.936	1351	3.018	33.436	40.461	1734	7.399	49.726	57.819	2096	16.944
Proposed	7.098	8.231	119	0.076	10.911	12.659	122	0.195	16.177	18.839	152	0.216	23.950	28.155	184	1.004	35.549	41.054	241	2.448

[a] Min.: Minimum PSL value (in dB). [b] Ave.: Average PSL value (in dB). [c] Time: Average time consumption (in seconds). [d] Iter.: Average number of conducted iterations.

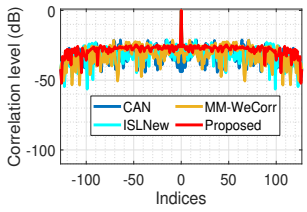

(a) Auto-correlation of the first waveform.

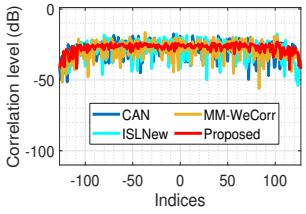

(b) Cross-correlation between the first and the second waveforms.

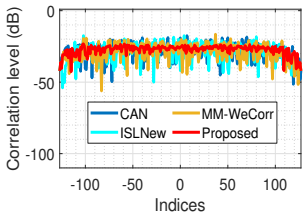

(c) Cross-correlation between the second and the first waveforms.

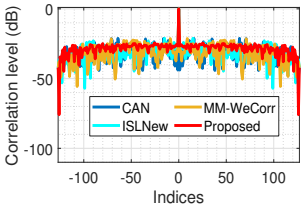

(d) Auto-correlation of the second waveform.

Fig. 2: Comparisons on the auto- and cross-correlation levels of waveforms generated by the tested algorithms.

tested code length $P = 2048$, which is approximately 4.759, 1.199, and 13.972 times less than the time consumptions of MM-PSL, ISLNew, and CAN, respectively.

V. Conclusions

We have proposed an efficient algorithm for designing multi-unimodular waveforms with low PSL toward any TLOI. The generic PSL metric defined on the TLOI is formulated for minimization via direct phase optimizations. Specifically, we first convert the PSL-minimization based design to an l_p-norm based minimization problem. Then, we reformulate it into an unconstrained optimization problem with respect to the phase values of waveform elements, wherein the inherent waveform property of constant envelopes and a DFT matrix are both used. Our remaining contributions lie in deriving the complex gradient of the unconstrained objective and elaborating its majorant via a Lipschitz-constant related quantity which is properly designed. A closed-form solution that updates the phase values through iterations is obtained using majorization-minimization techniques, which boils down to a gradient descent regime. The fast implementation of our proposed algorithm is also provided, whose performances have been verified to outperform current state-of-the-art methods.

References

[1] D. DeLong and E. M. Hofstetter, "On the design of optimum radar waveforms for clutter rejection," *IEEE Trans. Inf. Theory*, vol. 13, no. 3, pp. 454–463, Jul. 1967.

[2] N. Levanon and E.Mozeson, *Radar Signals*. Hoboken, NJ, USA: Wiley, 2004.

[3] M. C. Wicks, E. L. Mokole, S. D. Blunt, R. S. Schneible, and V. J. Amuso, *Principles of Waveform Diversity and Design*. Raleigh, NC, USA: SciTech Publishing, 2010.

[4] H. He, J. Li, and P. Stoica, *Waveform design for active sensing systems: A computational Approach*. Cambridge, UK: Cambridge University Press, 2012.

[5] D. Tse and P. Viswanath, *Fundamentals of wireless communication*. Cambridge, UK: Cambridge University Press, 2005.

[6] M. Nowak, M. Wicks, Z. Zhang, and Z. Wu, "Co-designed radar-communication using linear frequency modulation waveform," *IEEE Aerosp. Electron. Syst. Mag.*, vol. 31, no. 10, pp. 28–35, Oct. 2016.

[7] Y. Li, X. Wu, and R. Tao, "Waveform design for the joint MIMO radar and communications with low integrated sidelobe levels and accurate information embedding," in *IEEE Int. Conf. Acoust., Speech and Signal Process. (ICASSP)*, Toronto, ON, Canada, Jun. 2021, pp. 8263–8267.

[8] J. Li and P. Stoica, *MIMO Radar Signal Processing*. New York, NY, USA: Wiley, 2009.

[9] P. Stoica, H. He, and J. Li, "New algorithms for designing unimodular sequences with good correlation properties," *IEEE Trans. Signal Process.*, vol. 57, no. 4, pp. 1415–1425, Apr. 2009.

[10] J. Song, P. Babu, and D. P. Palomar, "Sequence set design with good correlations properties via Majorization-Mimimization," *IEEE Trans. Signal Process.*, vol. 64, no. 11, pp. 2866–2879, Jun. 2016.

[11] Y. Li and S. A. Vorobyov, "Fast algorithms for designing multiple unimodular waveforms with good correlation properties," *IEEE Trans. Signal Process.*, vol. 66, no. 5, pp. 1197–1212, Mar. 2018.

[12] X. Zhao, Y. Li, and R. Tao, "Efficent large-scale multi-unimodular waveform design with good correlation properties via direct phase optimizations," in *IEEE Int. Conf. Acoust., Speech and Signal Process. (ICASSP)*, Rhodes Island, Greece, Jun. 2023, pp. 1–5.

[13] Y. Li, C. Shi, and R. Tao, "Unimodular waveform design with low correlation levels: A fast algorithm development to support large-scale code lengths," in *IEEE Int. Conf. Acoust., Speech and Signal Process. (ICASSP)*, Singapore, May 2022, pp. 4983–4987.

[14] A. Aubry, A. D. Maio, and Y. Huang, "MIMO radar beampattern design via PSL/ISL optimization," *IEEE Trans. Signal Process.*, vol. 64, no. 15, pp. 3955–3967, Aug. 2016.

[15] J. Song, P. Babu, and D. P. Palomar, "Sequence design to minimize the weighted integrated and peak sidelobe levels," *IEEE Trans. Signal Process.*, vol. 64, no. 8, pp. 2051–2064, Apr. 2016.

[16] H. Esmaeili-Najafabadi, M. Ataei, and M. F. Sabahi, "Designing sequence with minimum PSL using Chebyshev distance and its application for chaotic MIMO radar waveform design," *IEEE Trans. Signal Process.*, vol. 65, no. 3, pp. 690–704, Feb. 2017.

[17] M. A. Kerahroodi, A. Aubry, A. D. Maio, M. M. Naghsh, and M. Modarres-Hashemi, "A coordinate-descent framework to design low PSL/ISL sequences," *IEEE Trans. Signal Process.*, vol. 65, no. 22, pp. 5942–5956, Jul. 2017.

[18] W. Fan, J. Liang, Z. Chen, and H. C. So, "Spectrally compatible aperiodic sequence set design with low cross- and auto-correlation PSL," *Signal Process.*, vol. 183, p. 107960, Jun. 2021.

[19] E. Raei, M. Alaee-Kerahroodi, P. Babu, and M. R. B. Shankar, "l_p-norm minimization of auto and cross correlation sidelobes in MIMO radars," in *23th Int. Radar Sympo.*, Gdansk, Poland, Sep. 2022, pp. 92–97.

[20] D. R. Hunter and K. Lange, "A tutorial on MM algorithms," *The American Statistician*, vol. 58, no. 1, pp. 30–37, Feb. 2004.

[21] Y. Nesterov, *Introductory Lectures on Convex Optimization: A Basic Course*. Boston: Springer Publishing Company, Incorporated, 2014.

[22] L. Hörmander, *The analysis of linear partial differential operators I: Distribution theory and Fourier analysis*. Berlin, Germany: Springer Publishing Company, 2015.